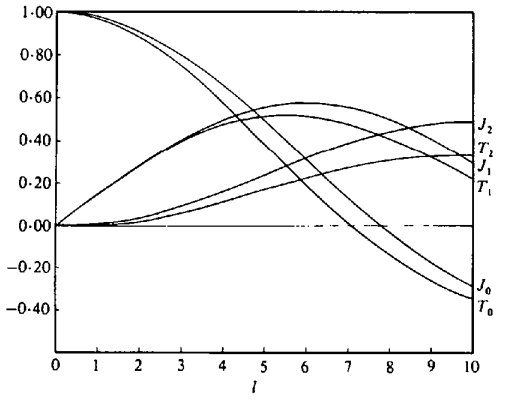

Fig. 1. The plot shows the influence of the phason factor upon the structure factor dependent on the reflexion index l. The functions $T_m(2\pi l.A_z, w_k^-)$ are calculated for the overall amplitude $A_z = 0{\cdot}05$ and for the overall phason factor $w_k^- = 0{\cdot}03$ Å^2. For $w_k^- = 0$ we get $T_m(2\pi l.A_z, 0) = J_m(2\pi l.A_z)$, the Bessel function of order m. The structure factor $F(hklm) = F(hkl) \times T_m(2\pi l.A_z, w_k^-)$.

significance of the R-factor improvements and confirm the model including a phason factor. For example, $R = 0{\cdot}487$ for 37 main reflexions $[I > 2\sigma(I)]$ of the layer $l = 6$ calculated without phason factors and $R = 0{\cdot}320$ for the refinement including phason factors. In comparison, the R factor of the same reflexions calculated from the refinement of the average structure is $R = 0{\cdot}501$. The corresponding R factors for the 58 second-order satellites $[I > 2\sigma(I)]$ of the layer $l = 2$ are $R = 0{\cdot}426$ and $R = 0{\cdot}314$, respectively. The main improvement in the description of the observed structure factors of these sensitive layers is therefore obtained by considering phase fluctuations. The generally high R factors can be explained by the fact that the peaked diffuse background under these weak Bragg reflexions cannot be separated very precisely by fitting the reflexion profiles with two Gaussian curves.

Conclusion

In this report the refinement of the displacively modulated structure of α-CuNSal was discussed under special consideration of the influence of phasons and amplitudons. In contrast to the results of the corresponding Ni phase (see part I) we have now obtained a significantly better description of the observed structure factors when including phason factors in our refinements. A possible explanation could be the higher temperature of investigation (270 K compared to 160 K for α-NiNSal) and therewith the existence of significant thermal effects like phasons and amplitudons. These results and the interpretation of the diffuse scattering (Adlhart *et al.*, 1982) are a reliable indication for the existence of fluctuations of phase and amplitude in the incommensurate phase of α-CuNSal.

We thank the Deutsche Forschungsgemeinschaft (DFG) for supporting this project (Project Ja15/34-35).

References

ADLHART, W., BLANK, H. & JAGODZINSKI, H. (1982). *Acta Cryst.* A**38**, 505–510.

International Tables for X-ray Crystallography (1974). Vol. IV. Birmingham: Kynoch Press.

STEURER, W. & ADLHART, W. (1983*a*). *Acta Cryst.* B**39**, 349–355.

STEURER, W. & ADLHART, W. (1983*b*). *Acta Cryst.* B**39**, 718–721.

WOLFF, P. M. DE, JANSSEN, T. & JANNER, A. (1981). *Acta Cryst.* A**37**, 625–636.

Acta Cryst. (1983). B**39**, 724–731

X-ray Study of Single Domains of 1,2-Dipalmitoyl-*sn*-phosphatidylcholine with less than 5% Water

BY J. DOUCET, A. M. LEVELUT AND M. LAMBERT

Laboratoire de Physique des Solides associé au CNRS, Université Paris-Sud, Bâtiment 510, 91405 *Orsay CEDEX, France*

(*Received* 2 *February* 1983; *accepted* 13 *June* 1983)

Abstract

Single domains of 1,2-dipalmitoyl-*sn*-phosphatidylcholine dihydrate ($C_{40}H_{80}NO_8P.2H_2O$) have been studied by X-ray scattering experiments. Some new information, which was not accessible by previous observations on powder samples, on the polymorphism of this compound is reported. A quantitative result concerning the molecular packing of the polar heads in the $L\delta$ phase has been deduced from the

0108-7681/83/060724-08$01.50

analysis of the diffuse scattering. The samples have been studied at atmospheric pressure or in vacuum in the temperature range 293–333 K, which corresponds to the crystalline phases and low-temperature lyotropic phases.

I. Introduction

The phospholipids are the major class of membrane lipids. The most common phospholipids found in the membranes of higher organisms are the phosphatidylcholines (lecithins). Their molecules are formed by two hydrophobic aliphatic chains linked on a hydrophilic head. These compounds exhibit a very rich and complex phase behaviour (% water–temperature) including crystalline phases and lyotropic phases characterized by quite different structures.

We present here an X-ray study of the crystalline and low-temperature lyotropic phases of 1,2-dipalmitoyl-*sn*-phosphatidylcholine (DPPC):

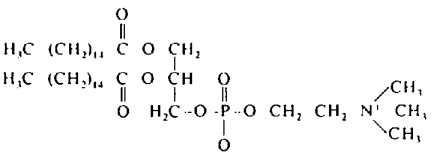

Unlike previous studies which have mostly been performed with powder samples, this study mainly deals with single-domain samples. This technique allowed us to obtain new three-dimensional results (such as the relative orientations of the lattices at the phase transitions) and also to observe diffuse scattering which provided important information about the structure of the lyotropic phases. Moreover, we found differences between heating the samples at atmospheric pressure and in vacuum; we report here the two sets of experiments.

II. Experimental

(*a*) *Preparation of the samples*

DPPC crystals were grown from a highly purified crystalline powder (Albon, 1977) in solution in chloroform and hexane. To remove traces of solvent without cracking the crystals, the samples were placed in a closed vessel for 24 h at normal pressure with high-vacuum oil to absorb vapour. The difference between the measured density and that calculated from our experimental lattice parameters assuming pure DPPC can be explained by the presence of a water content close to 4·8 wt %, which means that we have DPPC dihydrate. The crystals are platelet-shaped with an area of about 1 or 2 mm^2 and a thickness of a few hundred μm.

The lattice is orthorhombic with space group $P2_12_12_1$ and lattice parameters $a = 8{\cdot}87$, $b = 8{\cdot}99$, $c = 119{\cdot}9$ Å (Albon, 1976). There are eight molecules per unit cell. $|\mathbf{c}|$ corresponds to four molecular lengths and not two as expected since the molecules are arranged in such a way as to give a superstructure. Such a type of structure is different from the structures deduced from powder patterns of various lecithin samples (Pearson & Pascher, 1979) for which bilayer molecular packing is reported.

(*b*) *Powder device*

Powder patterns were recorded with a Guinier camera, equipped with an electric stage and using a focused monochromatic beam (Co $K\alpha_1$, λ = 1·7889 Å). As the samples, after one heating (up to 353 K)–cooling cycle, appear as 'plastic' sheets, they could be mounted on a wire mesh (platinum) which permitted heating. The initial crystalline sample could not be examined as it appeared undesirable to use any solvent in mounting. At room temperature, DPPC is evidently in equilibrium with air of average (laboratory) humidity (40–50%), but the water content can be varied slowly by humidity changes. At higher temperature there would be a more rapid loss of water. As exposure times for powder photographs were from 5 to 18 h, a change in the water content of the samples probably occurred.

(*c*) *Single-domain device*

We have obtained X-ray patterns with single-domain samples using a monochromatic beam (Cu $K\alpha$) diffracted by a doubly bent LiF crystal. The sample is fixed and the diffracted beams are collected on a flat film perpendicular to the direct beam. A brass oven surrounding the sample allows heating to 333 K. The collimator, the sample and the film are enclosed in an isolated atmosphere, the water content of which cannot be properly controlled. Two kinds of thermal conditions have been used:

– the sample is heated under vacuum;

– the sample is heated at atmospheric pressure and humidity.

These two treatments give different but individually reproducible results.

The purpose of this single-domain study was not to perform a precise structural determination but only to identify the different phases corresponding to a given treatment of the sample and to determine their symmetry.

The two techniques, powder method and single-domain method, are complementary. The powder method permits a precise determination of lattice parameters, thus providing information which is not always available by the single-crystal method.

(*d*) *Nomenclature of the 'phases' studied*

The phase sequence displayed by DPPC is complicated for three main reasons:

– it depends on the humidity;
– two 'phases' can appear simultaneously;
– large hysteresis effects occur on cooling.

Nevertheless, two different types of phases are observed: crystalline phases and lyotropic mesophases. The crystalline phases are exhibited in the 'crystalline region' which ranges up to 323 ± 10 K according to the external conditions. This 'crystalline region' on melting gives a lyotropic 'mesophase region'. On cooling this mesophase region remains metastable at room temperature for at least a few months. In the mesophase region we will refer to the nomenclature and classification of lecithin phases adopted by Luzzati, Gulik-Krzywicki & Tardieu (1968).

III. Crystalline region

The only information available in this region is given by the single-crystal study since the powder patterns were performed on previously heated samples which on decreasing the temperature are transformed into a metastable state different from the crystalline state.

As mentioned above, at room temperature under atmospheric pressure our single crystals display an orthorhombic structure. In Fig. 1(*a*) is presented an X-ray pattern of the **a*b*** reciprocal plane. The cell dimensions are such that the reflexions 200 and 120, which are the intense reflexions (surrounded by diffuse scattering), form a pseudo-hexagon since the reticular distances $d(200)$ and $d(120)$ are respectively equal to 4·43 and 4·01 Å.

When heated, new crystalline phases are exhibited. The nature of these phases depends on the pressure. We will give the results obtained by heating a crystal of DPPC.$2H_2O$ at atmospheric pressure and by heating it in a vacuum.

(*a*) *Heating at atmospheric pressure*

On heating the crystalline sample at atmospheric pressure a phase transition occurs at 323 K.

When the sample is irradiated 'perpendicularly'† to the layers, the well defined Bragg spots observed on the room-temperature pattern (Fig. 1*a*) disappear and are replaced by diffraction rings whose intensity is symmetrically modulated (Fig. 2*a*). The pattern obtained with the incident beam 'parallel' to the layers (Fig. 2*b*) indicates that the three-dimensional structure is maintained with the same orientation of the normal to the layers; only the orientation of the axes parallel to the layers is changed at the transition. It is possible to index the diffraction pattern of Fig. 2(*a*) corresponding to the **a* b*** reciprocal plane with a rectangular lattice of parameters $a \simeq 8{\cdot}8$ and $b \simeq 10{\cdot}1$ Å. These parameter lengths indicate that this phase is similar to the crystalline phase observed by Tardieu (1972). From the position of the intensity maxima on the rings, we can define the type of texture presented by this phase. The simplest way to describe the texture is to look at the most intense ring formed by the 200 and 120 reflexions. These reflexions which correspond nearly to the same reticular distance $d \simeq 4{\cdot}4$ Å are related to the pseudo-hexagonal packing of the aliphatic chains. This ring exhibits sixfold symmetry; it is formed by six arcs of circle of about 10° of extent and by six point

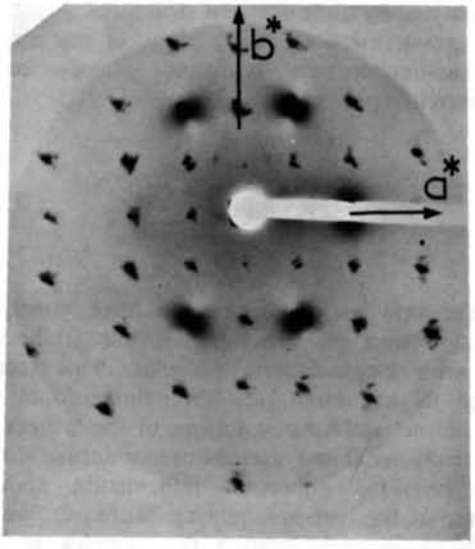

(*a*)

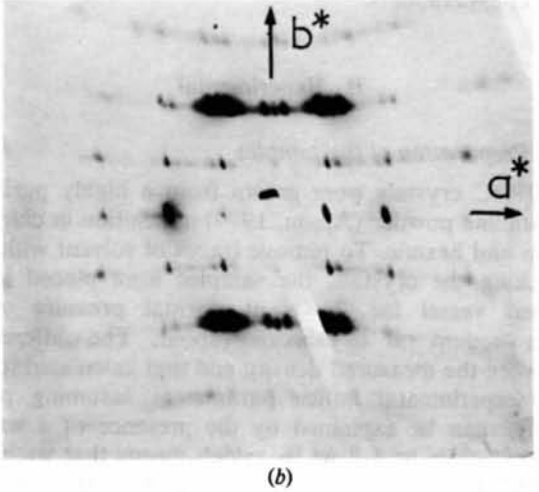

(*b*)

Fig. 1. Single-domain patterns. (*a*) Atmospheric pressure, **a* b***, $T \sim 293$ K. (*b*) Vacuum, **a* b***, $T \sim 293$ K.

† 'Perpendicularly' and 'parallel' respectively mean that the sample is oriented in order to obtain the **a* b*** plane or a plane containing **c***.

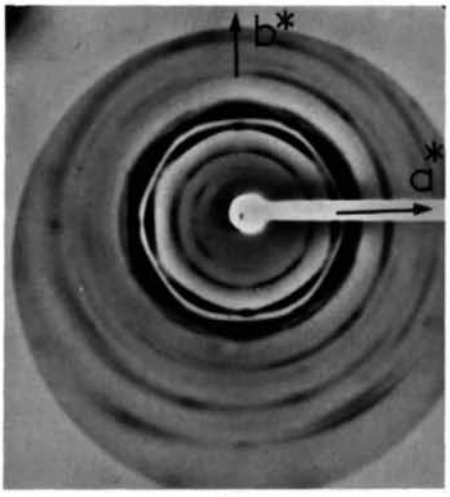

(*a*)

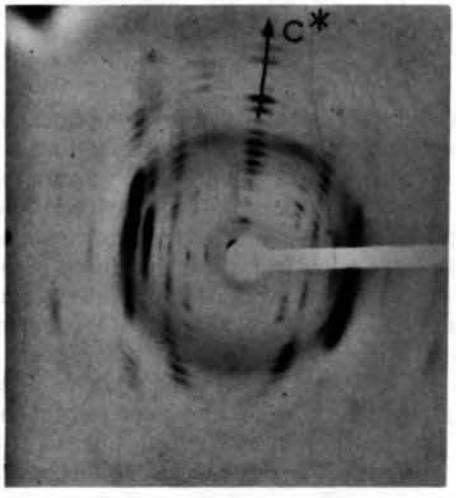

(*b*)

Fig. 2. Single-domain patterns when heating in the crystalline regions ($T \sim 330$ K). (*a*) X-ray beam perpendicular to the layers $\mathbf{a}^*\,\mathbf{b}^*$. (*b*) X-ray beam parallel to the layers.

reflections located at 30° from the middle of the arcs. Therefore, the pseudo-hexagonal lattice of the chain can adopt two kinds of orientation at the transition: in the first, one edge of the hexagonal lattice is more or less parallel to the [010] direction of the low-temperature form (arc reflexion of 10° of disorientation), whereas in the other this edge is strictly parallel to the [100] direction.

Let us note that any further heat treatment under atmospheric pressure ($T \leq 333$ K, upper limit of the heater device) leaves this crystalline form unchanged; the mesophase region is not reached.

(*b*) *Heating in a vacuum*

Under vacuum a small change occurs in the X-ray pattern of the form *B* of the crystals at room temperature. Satellite diffuse spots appear close to the layer lines perpendicular to $\mathbf{b}^*$ at a distance of about $\frac{1}{3}\mathbf{a}^*$ from the Bragg spots. Their intensity is high; two orders of satellites are detected around the most intense Bragg reflexions (Fig. 1*b*). These satellites disappear immediately when the sample returns to atmospheric pressure (Fig. 1*a*). The satellite pattern has not yet been extensively studied but is indicative of a change of the crystalline structure which occurs when the water is partially removed.

When heating under vacuum, no change in the X-ray pattern is detected below 313 K. At this temperature the crystal form *B* is directly transformed into a phase belonging to the mesophase region.

IV. Mesophase region

The description of the phases involved in the mesophase region is rather complicated since it depends on the temperature and also because various phases can appear simultaneously. The mesophase region has been observed in powder samples at atmospheric pressure and in single crystals heated in vacuum. A tentative explanation concerning the different behaviour between the powder and the single-crystal samples will be given in the *Conclusion*.

On heating a single crystal in a vacuum, a phase transition is detected at 313 K and another one at 323 K, while on heating the powder sample new diffraction rings appear as soon as 308 K, and from 323 up to 353 K the pattern aspect hardly changes.

(*a*) *Single domain heated in a vacuum* ($T < 323$ K)

Let us begin with the description of the single-crystal patterns. Before heating, the crystal is in its orthorhombic form and its pattern exhibits additional satellite reflections (Fig. 1*b*).

At 313 K most of the crystalline Bragg spots disappear. When the X-ray beam is parallel to the **c** direction of the crystalline form, the new pattern exhibits point-like reflexions plus continuous powder rings (Fig. 3*a*). The six Bragg spots correspond in real space to a pseudo-hexagonal lattice of parameter length $a = 5{\cdot}1$ Å which is oriented in the same way as the pseudo-hexagon formed by the intense Bragg spots in the previous crystalline form. The rings originate from a square lattice of cell dimension $a \simeq 6{\cdot}7$ Å (indices 100, 110). The patterns obtained with the beam perpendicular to **c** (Fig. 3*b*) do not exhibit any Bragg reflexion out of the equatorial plane except along the $\mathbf{c}^*$ direction, but only diffuse lines parallel to $\mathbf{c}^*$, the intensity of which is strongly modulated along $\mathbf{c}^*$. This pattern is typical of a layered structure formed by a stacking of two-dimensional ordered layers without correlation between successive layers.

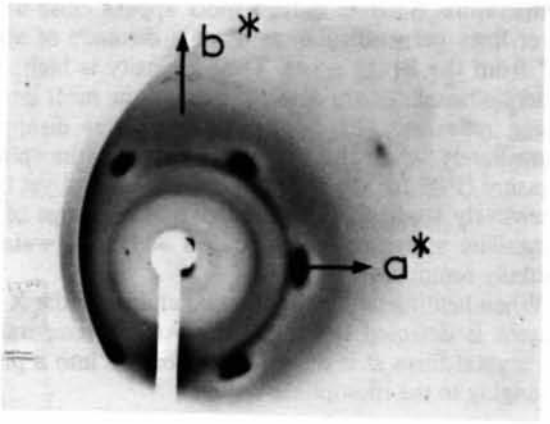

(*a*)

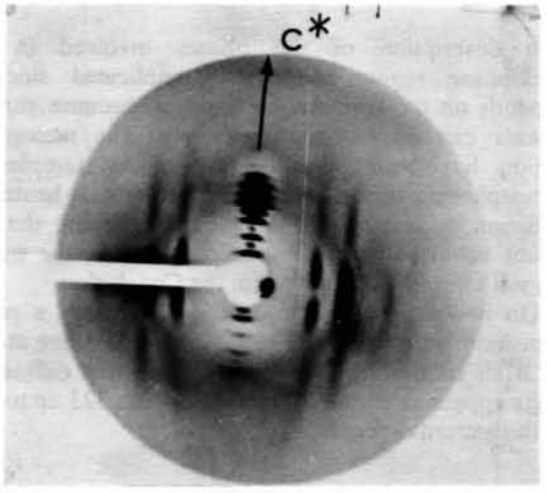

(*b*)

Fig. 3. Single-domain patterns of a heated crystal in the mesophase region 313 K. (*a*) X-ray beam perpendicular to the layers. The inner ring corresponds to the intersect of the Ewald sphere with the diffuse crystalline cylinder ($10S_z$); this intersect is not exactly located in the plane **a*** **b*** which explains why it is observed. (*b*) X-ray beam parallel to the layers.

We can give an explanation of these patterns involving two kinds of domains. The pseudo-hexagonal one seems to correspond, using the notation of Tardieu, Luzzati & Reman (1973), to an $L\beta'$ phase with a unique orientation of the hexagonal lattice in the whole sample. In this type of phase the molecules are packed into layers with their long axes parallel and within each layer the long axes are located at the nodes of an hexagonal lattice. They are inclined on the layers: on a complementary picture we detect at least two different orientations of the aliphatic chains (**c**) forming an angle of $15 \pm 5°$ with the normal direction to the layer plane.

The square lattice corresponds to a non-oriented $L\delta$ phase. This phase has a bilayered structure in which the polar heads are distributed on a square lattice of edge

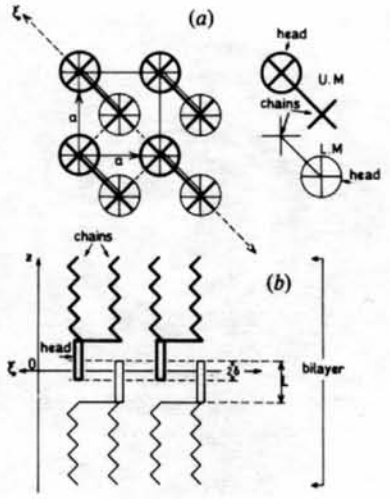

Fig. 4. Schematic representations of the $L\delta$ phase structure. (*a*) **a b** plane. (*b*) (**a** + **b**)**c** plane. UM upper-level, LM lower-level molecule.

$\simeq 6{\cdot}7$ Å and the chains, which are somewhat distorted and stand perpendicularly to the layers, on a square lattice of edge $(a\sqrt{2})$ tilted by 45° from the head lattice. The polar heads of two adjacent layers are interdigitated as shown in Fig. 4: in projection onto the layer plane the polar heads and the chains of the same bilayer form a centred square lattice of parameter a.

The diffuse lines observed in Fig. 3(*b*) come from the $L\delta$ phase. They are the intersects of cylinders of axis parallel to **c*** with the Ewald sphere. From the intensity modulation along **c*** we can test the model of the $L\delta$ phase presented by Tardieu, Luzzati & Reman (1973). According to this model, the structure factor along the hkS_z diffuse-scattering cylinders (where S_z is the scattering-vector component along **c***) must be equal to zero for $S_z = 0$ when $(h + k)$ is odd. This is in agreement with the pattern Fig. 3(*b*) in which the intensity on the cylinders $10S_z$ and $21S_z$ is equal to zero for $S_z = 0$, whereas we have no extinction for this value of S_z on the $11S_z$ and $20S_z$ cylinders. Now, the chain thickness in the bilayer being large compared to the head thickness, the chain contribution to the scattering intensity mainly lies near the equatorial plane **a*** **b***. Thus the intensity corresponding to high values of S_z along **c*** mainly proceeds from the polar heads. From the intensity modulation along the reflexions $10S_z$ and $11S_z$ we can deduce two geometrical parameters characterizing the packing, the polar-head length L and the depth of interpenetration of the polar heads 2δ (Fig. 4).

For this let us call z the axis parallel to the molecular axes **c** and O the origin located at the middle of the polar-head part of the bilayer. We intend to calculate the contribution to the structure factor due to the polar heads. We choose the simple approximation in

which the polar heads are assimilated to linear continuous rods of homogeneous electron density oriented along z, the positions of which in the unit cell are $(x = 0, y = 0)$ and $(x = \frac{1}{2}, y = \frac{1}{2})$ when referring to the square lattice of parameters $a \simeq 6{\cdot}7$ Å. Thus, the structure factor can be written:

$$F(h,k,S_z,\delta) = \rho\left[\int_{-L+\delta}^{\delta} \exp(2i\pi S_z z\,dz) + \exp i\pi(h+k) \times \int_{-\delta}^{L-\delta} \exp(2i\pi S_z z\,dz)\right],$$

where S_z is the scattering-vector component along the z direction.

For $h + k = 2n$, it takes the form:

$$F(S_z,\delta) = -\frac{\rho}{\pi S_z}(\sin\pi)\,S_z L\,(\cos\pi)\,S_z(L-2\delta).$$

For $h + k = 2n + 1$, it takes the form:

$$F(S_z,\delta) = \frac{i\rho}{\pi S_z}(\sin\pi)\,S_z L\,(\sin\pi)\,S_z(L-2\delta).$$

The variation of the corresponding intensity as a function of S_z is represented in Fig. 5.

Experimentally, mainly two sections of the reciprocal cylinders of scattering of axes **c*** are visible: the inner one is the $10S_z$ and the second is the $11S_z$. The intensity distribution of $10S_z$ is consistent with the calculated profile for $(h + k)$ odd: it is equal to zero for $S_z = 0$ and the first minimum when increasing S_z gives us the value of $1/L$, *i.e.* $L \simeq 9{\cdot}5 + 1$ Å. The second reflexion $11S_z$ is also consistent with the calculated profile for $(h + k)$ even, since it is a maximum for $S_z = 0$ and is roughly equal to zero for values of S_z between $1/2(L - 2\delta)$ and $1/L$, which gives $2\delta \simeq 3{\cdot}7 \pm 0{\cdot}5$ Å. Thus our simple structure-factor calculation is consistent with the intensity modulation displayed by the reflexions hkS_z of the $L\delta$ phase in the hypothesis of an interpenetration of the polar heads, at least for values of S_z slightly larger than $1/L$; the value of L is quite consistent with the partial volume of the glycerophosphorylcholine and carboxylic groups (360 Å^3) (Tardieu, 1972).

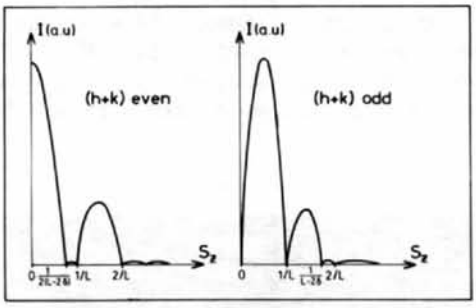

Fig. 5. Schematic representation of the intensity along the diffuse cylinders in the $L\delta$ phase.

(*b*) *Single crystal heated in vacuum* ($323 < T < 333$ K)

At 323 K, the pattern aspect changes (Fig. 6*a*,*b*). The diffuse cylindrical reflections parallel to **c*** break out into Bragg spots, which indicates the establishment of three-dimensional ordering (Fig. 6*b*): the previous two-dimensional $L\delta$ ($L\delta$–2D) domains are transformed into domains characterized by a three-dimensional order ($L\delta$–3D). Simultaneously, in the reciprocal plane perpendicular to **c** each ring splits into twelve well defined spots (Fig. 6*a*). So the hexagonal structure of the sample ($L\delta'$) seems to be unchanged while the $L\delta$ part is transformed into a three-dimensional quadratic lattice and a well defined relation exists between the two phases.

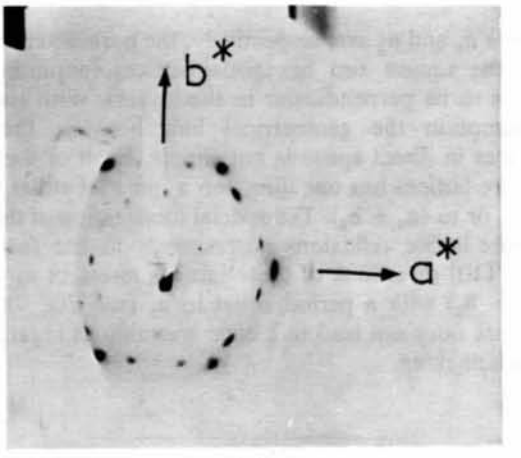

(*a*)

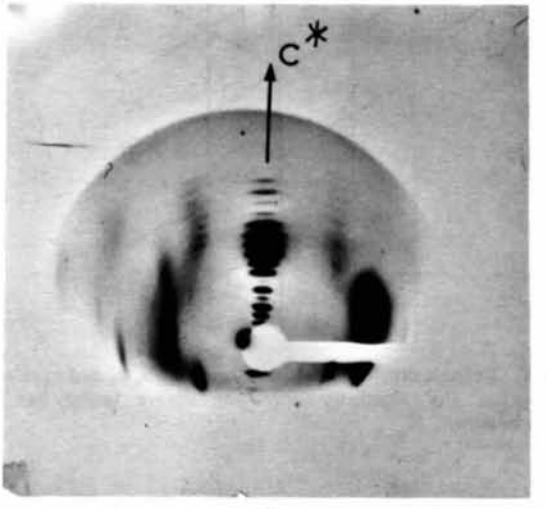

(*b*)

Fig. 6. Single-domain patterns in the mesophase region at 323 K under vacuum. (*a*) X-ray beam perpendicular to the layers and its schematic representation. The inner reflexions are in fact the 101 reflexions and not the 100 which have zero intensity. (*b*) X-ray beam parallel to the layers.

In the reciprocal plane $\mathbf{a}^*$ $\mathbf{b}^*$ the 110 spots proceeding from the square lattice seem to be located on the edges of the hexagon formed by the reflexions 100 and 010 and its homologues of the β' phase. There are three orientations for the square lattice which correspond to the three orientations of the edges of the hexagon. If we call e_h^* and e_c^* respectively the edge lengths of the hexagon and of the square in reciprocal space, and if we assume that the square-lattice reflexions are exactly located on the edges of the hexagon, we have the relation:

$$e_c^* = e_h^*(3 - \sqrt{3}).$$

The corresponding relation in direct space is:

$$a_c = \frac{\sqrt{3} + 1}{2} a_h \simeq 1{\cdot}366\, a_h$$

where a_c and a_h are, respectively, the parameter lengths for the square and hexagonal lattices (assuming the chain to be perpendicular to the layers). With such an assumption the geometrical link between the two lattices in direct space is not simple. Each of the three square lattices has one direction $\mathbf{a}_c$ parallel either to $\mathbf{a}_h$, to $\mathbf{b}_h$ or to $(\mathbf{a}_h + \mathbf{b}_h)$. The special localization of the 110 square-lattice reflexions corresponds to the fact that the [110] directions of these lattices intersect $\mathbf{a}_h$, $\mathbf{b}_h$ or $(\mathbf{a}_h + \mathbf{b}_h)$ with a period equal to $\mathbf{a}_h$ (see Fig. 7). This remark does not lead to a clear meaning as regards the chain packing.

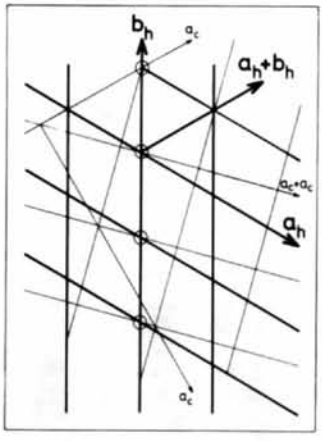

Fig. 7. Relative orientations of the hexagonal $\mathbf{a}_h$ $\mathbf{b}_h$ and square $\mathbf{a}_c$ $\mathbf{a}_c$ lattices. For simplicity only one square lattice has been represented.

We think it more probable that the length–parameter relation is only fortuitous for the following reason: assuming that the area per chain is the same for the two lattices, we have $a_c/a_h = 1{\cdot}316$, which is close to 1·366. Experimentally, we find from the more precise powder data (see § IV*c*) $a_c/a_h = 1{\cdot}321$, which corresponds to a chain-area difference lower than 1%. With such a value, the 110 square-lattice reflexions seem to be aligned with the hexagonal-lattice reflexions. In conclusion, we can assume that, the chain area for the two lattices being almost equal, the two packings correspond to neighbouring free enthalpy, which accounts for the simultaneous presence of the two lattices. This leads to four types of domains, the orientation of the three square domains being determined by the hexagonal domain.

(*c*) *Powder sample heated in atmospheric pressure*

Let us now compare these results obtained from the single-crystal patterns with those given by the powder patterns.

When heating, new rings appear on the powder pattern at about 308–313 K, and the pattern aspect does not change from 323 up to 353 K. The study of our powder patterns (Fig. 8) confirms the single-crystal study and permits new information concerning the structure of the $L\delta$–3D domains to be obtained. The rings can be explained by the simultaneous presence of hexagonal and square lattices.

According to the sample thermal treatment, the hexagonal domains give either only one diffraction ring in the range 4–5 Å (it probably corresponds to an $L\beta'$ phase) or a few rings probably indicating the presence of a domain with a higher degree of order, perhaps a three-dimensional $L\beta'$ domain.

The structure of the domain with the square lattice also depends on the sample thermal treatment: according to the conditions, two types of cells can be observed, but we cannot predict which will appear. For both types, the rings (110) and (200) are present on the powder patterns. In the range 7–6 Å a few rings are also visible. For the first cell type, they are indexed as the 101, 102, 103, 104 reflexions of a primitive tetragonal cell assuming that the layer thickness $|\mathbf{c}|$ is equal to the observed distance $\simeq 54$ Å; for the second cell type, they are indexed as 101, 103, 105, 107 reflexions with $|\mathbf{c}| \simeq 107$ Å (Table 1), that is to say with a body-centred tetragonal cell. These three-di-

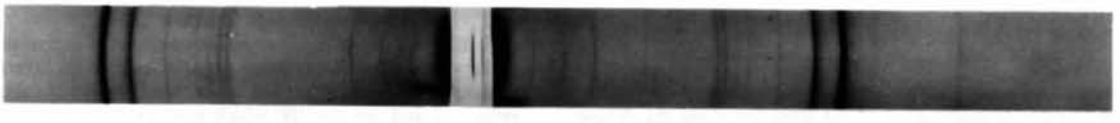

Fig. 8. X-ray powder pattern of DPPC in the mesophase region (348 K).

Table 1. *List of the measured (d_m) and calculated (d_c) reticulated distances for the Lδ–3D* phase of *DPPC (body-centred tetragonal : $a = b = 6{\cdot}788$, $c = 106{\cdot}8$ Å)*

$h\,k\,l$	d_m (Å)	d_c (Å)
0 0 2	53·5 ± 0·2	53·40
0 0 1	47·2 ± 0·2	
0 0 4	26·7 ± 0·1	26·70
0 0 6	17·80 ± 0·05	17·80
0 0 8	13·36 ± 0·02	13·35
1 0 1	6·774 ± 0·01	6·774
1 0 3	6·670 ± 0·01	6·670
1 0 5	6·467 ± 0·008	6·465
1 0 7	6·193 ± 0·008	6·194
0 0 18	5·927 ± 0·006	5·933
0 0 20	5·338 ± 0·006	5·340
0 0 22	4·857 ± 0·005	4·854
1 1 0	4·797 ± 0·005	4·798
0 2 0 (Lβ')	4·448 ± 0·005	
2 0 0	3·394 ± 0·004	3·394

mensional domains are the Lδ–3D domains which appear at 323 K on heating a single crystal in vacuum. It is the first time that a three-dimensional Lδ domain is encountered. It is interesting to note that the bilayer thickness of 54 Å is significantly larger than the previously reported value for the Lδ phase of DPPC $\simeq$ 47 Å (Tardieu, 1972). Nevertheless, that value of 47 Å also appears on a few patterns. Then, we probably have a mixture of Lδ–2D and Lδ–3D domains. The establishment of the three-dimensional order seems connected to a change of the aliphatic-chain packing or of the depth of interpenetration 2δ of the polar heads.

Conclusion

In the dry region of the diagram (T, % water) the dipalmitoylphosphatidylcholine exhibits a complex behaviour. This behaviour seems reproducible in spite of some differences observed on the X-ray patterns of samples which have been submitted to slightly different thermal treatments. These differences can probably be attributed to very important supercooling effects and to the fact that two phases can be simultaneously present. The sample purity and the solvent evaporation also seem to be important factors, especially as regards the degree of the crystallographic order. From the single-domain patterns we have deduced the depth of interpenetration of the polar heads in the Lδ phase (3·7 ± 0·5 Å). We have shown that with very pure solvent-free samples, we obtain domains similar to the Lδ phase but characterized by a *three-dimensional order* instead of a two-dimensional as previously reported. This new type of lecithin phase has been observed on both powder and single-domain X-ray patterns. The single-domain study has also permitted the mutual orientation between the various phases to be determined and the structural parameters of the Lδ–2D domains to be deduced from the diffuse-scattering study. Moreover, a coupling between bilayers in the Lδ–3D phase has been detected by the powder study. The small differences between the powder samples and the single-domain behaviour are probably due to the fact that the water content is not controlled and thus not precisely known. When heating a single domain, the water evaporation may be hindered since the water molecules have to diffuse to the surface. This process is accelerated either in vacuum or by using a powder in which the size of the domains is not a hindrance for the water evaporation. This explanation accounts for the nearly similar behaviour of a single domain in vacuum and of a powder sample. The differences between the transition temperatures of DTA and X-ray samples are also probably due to different water contents.

Finally, we wish to point out that for these 'ordered' lecithin phases, the molecular packing seems to be governed by the aliphatic-chain packing rather than by the polar-head packing, or at least we can say that the head packing does not always clearly appear on the X-ray pattern whereas the chain packing is always present. The pseudo-hexagonal lattice corresponding to reticular distances of about 4·2 Å, *i.e.* of chain–chain distances, persists in all the phases from the crystalline phases up to the (Lδ–3D)–Lβ' mixture where it determines the orientations of the Lδ–3D domains.

The structures exhibited by lecithins appear to be very complex and highly dependent on the external conditions. Further investigations on these compounds would need a good control of all the factors contributing to the molecular-arrangement determination.

The authors wish to thank Dr N. Albon for providing the single crystals of lecithins and for many helpful discussions.

References

ALBON, N. (1976). *J. Cryst. Growth*, **35**, 105–109.
ALBON, N. (1977). *J. Cryst. Growth*, **42**, 249–252.
LUZZATI, V., GULIK-KRZYWICKI, T. & TARDIEU, A. (1968). *Nature (London)*, **218**, 1031–1034.
PEARSON, R. H. & PASCHER, I. (1979). *Nature (London)*, **281**, 499–501.
TARDIEU, A. (1972). Thèse de doctorat d'état, Univ. Paris-Sud N° 915.
TARDIEU, A., LUZZATI, V. & REMAN, F. C. (1973). *J. Mol. Biol.* **75**, 711–733.